中國機械工程學刊第四十四卷第一期第 37~48 頁(民國一百一十二年)
Journal of the Chinese Society of Mechanical Engineers, Vol.44, No.1, pp 37~48 (2023)

Mathematical Modeling of Flexible Robot Manipulators with Slender Links – a Lumped Parameter Approach

Chung-Chan Hsu**, Hao-Lun Huang**, Chang-Fu Lu** and Ming-Yang Cheng*

Keywords： Flexible Robot Manipulator, Euler-Bernoulli Equation, Euler-Lagrange Equation, Lumped Parameter Method.

ABSTRACT

Robot manipulators with flexible links are made of light materials with low rigidity/stiffness. On one hand, low rigidity makes the flexible robot manipulator safer than the rigid robot manipulator during operation. On the other hand, low rigidity also results in vibration occurring at the endpoint of the flexible link. As a result, the motion accuracy of the flexible robot manipulator is often much worse than that of the rigid robot manipulator. One effective way to deal with the vibration problem is to design a model-based control scheme. Consequently, this paper aims at conducting an in-depth study on the derivation of the mathematical model of the flexible robot manipulator with slender links made of uniform materials. In particular, the Euler-Bernoulli equation, the Euler-Lagrange equation, and the lumped parameter method are employed in deriving the mathematical model. Several experiments and computer simulations have been conducted. Experimental results indicate that the discrepancy between the natural frequency obtained from the real single-link flexible robot manipulator and that of the mathematical model derived using the proposed approach is very small. In addition, results of computer simulations verify the effectiveness of the proposed approach.

INTRODUCTION

Robot manipulators with flexible links are made of light materials with low rigidity/stiffness. Since the flexible links are lighter than the rigid links, compared with the rigid robot manipulator, the required power of the servomotors that actuate the flexible robot manipulator can be smaller, resulting in lower cost and less energy consumption. In addition, the mass and inertia of the flexible link are smaller; as such, the possibility of endangering the safety of users/operators is less likely.

However, low rigidity results in vibration occurring at the endpoint of the flexible link. As a result, the motion accuracy of the flexible robot manipulator is often much worse than that of the rigid robot manipulator. To facilitate the use of flexible robot manipulators, finding an effective way to deal with the vibration problem is essential. One of the promising approaches to cope with the aforementioned problem is the model-based control scheme. As a result, this paper aims at conducting an in-depth investigation on issues related to the kinematics and dynamics of the flexible robot manipulator. In particular, the Euler-Bernoulli equation, the Euler-Lagrange equation, and the lumped parameter method are employed in deriving a mathematical model for the flexible robot manipulator with slender links made of uniform materials.

According to the past studies in flexible robot manipulators (Book, 1990; Theodore & Ghosal, 1995; Dwivedy & Eberhard, 2006; Zhang et al., 2007; Gao & Wang, 2012; Lochan et al., 2016; Sharifnia & Akbarzadeh, 2017; Meng et al., 2018), in addition to the kinematic energy generated by the motion, various types of potential energy can be stored in robot joints (i.e. servomotor, harmonic drive and spring), transmission components (i.e. belt) and links. In particular, the compliance caused by a joint can be approximated by a spring. In addition, due to its low moment of inertia, the transmission component can be approximated by a lumped spring. In general, the forces due to a link include torsion, bending and compression. This paper only considers the bending force of a flexible link.

The Timoshenko beam equation and the Euler-Bernoulli equation (Theodore & Ghosal, 1995; Meirovitch, 1997; Tokhi & Azad, 2008) are two of

Paper Received January, 2022. Revised December, 2022. Accepted January, 2023. Author for Correspondence: Ming-Yang Cheng.

** Graduate Student, Department of Electrical Engineering, National Cheng Kung University, Tainan, Taiwan 701, ROC.*
*** Professor, Department of Electrical Engineering, National Cheng Kung University, Tainan, Taiwan 701, ROC.*

the most popular approaches in studying the mathematical model of the deformation of a flexible link. Since the Timoshenko beam equation takes into account the link's shear force, it is more suitable for studying the case of a short and thick flexible link that has a significant shear force (Gao & Wang, 2012). In contrast, the Euler-Bernoulli equation is more suitable for studying the case of a slender link. In this case, the shear force is very small and can be neglected. Since the flexible link investigated in this paper is slender, the Euler-Bernoulli equation is adopted in this paper.

The commonly used approaches for solving the Euler-Bernoulli equation are the Finite Element Method (FEM) (Theodore & Ghosal, 1995; Sharifnia & Akbarzadeh, 2017), the Assumed Mode Method (AMM) (Theodore & Ghosal, 1995; Sharifnia & Akbarzadeh, 2017) and the lumped parameter method (Sakawa et al., 1985; Hastings & Book, 1987; Benati & Morro; 1988; Chapnik, et al., 1991; Luca & Siciliano, 1991; Feliu, et al., 1992; Matsuno et al., 1994; Ge et al., 1997; Zhu et al., 1999; Subudhi & Morris, 2002; Martins et al., 2003; Faris et al., 2009; Sun et al., 2017; Hong et al., 2017). Among the above three methods, the lumped parameter method requires the least computation resources. In particular, when using the lumped parameter method, the energy caused by the deformation of the flexible robot manipulator is approximated by the energy generated by a system consisting of a point mass, a spring and a damper. The modeling accuracy of the lumped parameter method may not be as good as the other two methods; nevertheless, its computation time is shorter and may prove to be a big advantage over the other two methods in practice.

In addition to studying the deformation of a flexible link, this paper also investigates the forward kinematics and differential kinematics of the flexible robot manipulator. For a flexible robot manipulator of low degree-of-freedom, one can exploit the geometric relations and trigonometric functions to study forward kinematics and differential kinematics. However, it will be very difficult, if not impossible, for high dimensional cases. In this paper, the popular *Denavit–Hartenberg* (DH) parameters (Denavit & Hartenberg, 1955; Fu et al., 1987) are exploited to cope with high dimensional cases. In particular, this paper introduces a coordinate transformation matrix that takes into account the deflection due to the deformation in all directions. By combining the coordinate transformation matrix introduced in this paper with the coordinate transformation matrix suitable for the rigid robot manipulator defined by the DH parameters, one can construct the kinematics model for a general flexible robot manipulator.

The rest of the paper is organized as follows. Section 2 introduces the mathematical model for describing the deformation of the flexible robot manipulator. Section 3 derives the kinematics model, while the dynamic model is obtained in Section 4. Simulation and experimental results are provided in Section 5. Conclusions are given in Section 6.

MODELING OF THE DEFORMATION OF THE FLEXIBLE ROBOT MANIPULATOR

In this section, the mathematical model for describing the deformation of the flexible robot manipulator will be derived.

Euler-Bernoulli equation

In this paper, the Euler-Bernoulli equation that ignores the effects of torsion and shear force is used to describe the deformation of the flexible link. Fig. 1 illustrates two typical one-link flexible robots—the revolute joint and the prismatic joint. Fig. 2 shows the deflection of the position of the endpoint for a revolute-type flexible robot manipulator due to deformation.

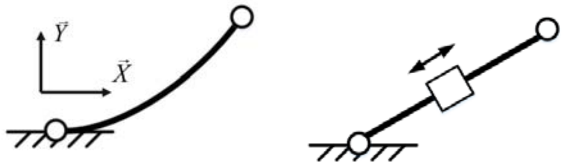

Fig. 1. Typical single-link flexible robots (left: revolute joint; right: prismatic joint).

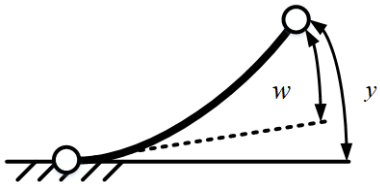

Fig. 2. Deflection of the position of the endpoint for a revolute-type flexible robot manipulator due to deformation (y: displacement of the endpoint from the horizontal axis; w: deflection due to deformation).

Eq. (1) is the partial differential equation that describes the relationship between the deflection $w_i(x,t)$ of the endpoint of a flexible link due to deformation and time t, as well as position x.

$$\begin{cases} E_i I_i \dfrac{\partial^4 w_i(x,t)}{\partial x^4} + \rho_i \dfrac{\partial^2 w_i(x,t)}{\partial t^2} = -\rho_i x \theta_i = \tau_{ext,i} \\ \text{for direction of revolute control force of } i\text{-th axis} \end{cases}$$
$$\begin{cases} E_i I_i \dfrac{\partial^4 w_i(x,t)}{\partial x^4} + \rho_i \dfrac{\partial^2 w_i(x,t)}{\partial t^2} = 0 \\ \text{otherwise} \end{cases} \tag{1}$$

where x: position; t: time; E_i: Young's modulus of the i^{th} link; I_i: second axial moment of area of the i^{th} link; E_iI_i: rigidity of the i^{th} link; ρ_i: linear density of the i^{th} link.

The total displacement $y_i(x,t)$ of a point x of the i^{th} link in the world frame, i.e. the sum of the movement by the rigid link and the deformation due to flexibility, can be expressed as Eq. (2).

$$y_i(x,t) = \begin{cases} \left\langle \begin{array}{l} x\theta_i(t) + w_i(x,t) \\ \text{for direction of revolute control force of } i\text{-th axis} \end{array} \right. \\ \left\langle \begin{array}{l} w_i(x,t) \\ \text{otherwise} \end{array} \right. \end{cases} \quad (2)$$

For the revolute-type flexible manipulator shown in Fig. 1, the displacement on the Z-axis (outward of the paper) is $x\theta+w_y$, while the displacement on the X-axis and Y-axis are w_z and w_x, respectively. For the prismatic-type flexible manipulator shown in Fig. 1, the displacement on the X-axis, Y-axis and Z-axis are w_x, w_y and w_z, respectively.

As pointed out in (Matsuno et al., 1994), the boundary conditions for the forced Euler-Bernoulli equation (i.e. with external force) are very complicated. As a result, most existing literatures focus on the case of an unforced Euler-Bernoulli equation. Namely, only the boundary conditions for the case of free vibration will be considered in this paper. Note that the mathematical model derived using the unforced Euler-Bernoulli equation cannot accurately describe the dynamic behavior of the flexible link under large external force. Nevertheless, for application scenarios such as pick-and-place tasks, one of the most important issues is to suppress vibration after the target position is reached. It is conceivable that the control force (i.e. external force) after the target position is reached is much smaller than that for a flexible link in motion. Therefore, the mathematical model derived using an unforced Euler-Bernoulli equation can be used to describe the dynamic behavior of the flexible link in a pick-and-place task without sacrificing too much accuracy. For the case of free vibration, Eq. (1) can be rewritten as Eq. (3):

$$E_i I_i \frac{\partial^4 w_i(x,t)}{\partial x^4} + \rho_i \frac{\partial^2 w_i(x,t)}{\partial t^2} = 0 \text{ for } i\text{-th axis} \quad (3)$$

Lumped parameter method

According to (Hastings & Book, 1987; Benati & Morro; 1988; Chapnik, et al., 1991; Luca & Siciliano, 1991; Matsuno et al., 1994; Subudhi & Morris, 2002; Martins et al., 2003; Faris et al., 2009), the boundary conditions of the Euler-Bernoulli equation for the case of external load can be described by Eqs. (4)-(6):

$$w_i(x,t)\big|_{x=0} = 0 \quad , \quad \frac{\partial w_i(x,t)}{\partial x}\Big|_{x=0} = 0 \quad (4)$$

$$E_i I_i \frac{\partial^3 w_i(x,t)}{\partial x^3}\Big|_{x=L_i} = M_{p_i} \frac{d^2}{dt^2}\big[w_i(x,t)\big]\Big|_{x=L_i} \quad (5)$$

$$E_i I_i \frac{\partial^2 w_i(x,t)}{\partial x^2}\Big|_{x=L_i} = -I_{p_i} \frac{d^2}{dt^2}\left(\frac{\partial w_i(x,t)}{\partial x}\right)\Big|_{x=L_i} \quad (6)$$

where index i represents the i^{th}-axis, M_{p_i} is the mass of payload for the i^{th}-axis, and I_{p_i} is the moment of inertia of payload for the i^{th}-axis.

With the boundary conditions given by Eq. (4)-(6), one can solve Eq. (3) and yield the following transcendental equation for β_{ij}.

$$\begin{aligned} 0 = {} & 1 + \cosh\beta_{ij}L_i \cos\beta_{ij}L_i + \frac{M_{p,i}}{\rho_i L_i}\beta_{ij}\begin{pmatrix} \sinh\beta_{ij}L_i\cos\beta_{ij}L_i \\ -\cosh\beta_{ij}L_i \sin\beta_{ij}L_i \end{pmatrix} \\ & - \frac{I_{p,i}\beta_{ij}^{\ 3}}{\rho_i L_i^{\ 3}}\left(\sinh\beta_{ij}L_i\cos\beta_{ij}L_i + \cosh\beta_{ij}L_i\sin\beta_{ij}L_i\right) \\ & + \frac{M_{p,i}I_{p,i}\beta_{ij}^{\ 4}}{\rho_i^{\ 2}L_i^{\ 4}}\left(1 - \cosh\beta_{ij}L_i\cos\beta_{ij}L_i\right) \end{aligned} \quad (7)$$

where index i represents the i^{th}-axis and j represents the j^{th} mode of the flexible link.

By solving Eq. (7) for β_{ij}, the resulting eigenfunction F_{ij} (x) can be found (Sakawa et al., 1985; Sun et al., 2017).

$$F_{ij}(x) = \frac{1}{\kappa_{ij}}\begin{bmatrix} \cosh\beta_{ij}x - \cos\beta_{ij}x \\ -\dfrac{\cosh(\beta_{ij}L_i) + \cos(\beta_{ij}L_i)}{\sinh(\beta_{ij}L_i) + \sin(\beta_{ij}L_i)}\left(\sinh\beta_{ij}x - \sin\beta_{ij}x\right) \end{bmatrix} \quad (8)$$

where

$$\kappa_{ij} = \int_0^{L_i} F_{ij}(x)^2 dx = \begin{cases} \left[L_i + \dfrac{\rho_i L_i^{\ 2}}{M_{p,i}\beta_{ij}^{\ 2}}\left(\dfrac{1+\cosh\beta_{ij}\cos\beta_{ij}}{\sinh\beta_{ij}\sin\beta_{ij}}\right)^2\right]^{\frac{1}{2}} \\ \sqrt{L_i} \quad \text{if } M_{p,i} = 0 \end{cases}$$

In addition, according to (Feliu, et al., 1992; Ge et al., 1997; Zhu et al., 1999; Hong et al., 2017; Sun et al., 2017), the kinetic energy due to the deformation of the i^{th} link can be expressed as

$$T_{e,i} = \frac{1}{2}\rho_i\int_0^{L_i}\dot{w}_i^{\ 2}dx \quad , \quad T_e = \sum_{i=1}^{n} T_{e,i} \quad (9)$$

where n: the total number of links; T_e: total kinetic energy of all flexible links; $T_{e,i}$: kinetic energy of the i^{th} flexible link.

In the case of free vibration for the Euler-Bernoulli equation, the rigid displacement due to control force is zero. As a result, we have y_i=w_i.

Using the 1st order assumed mode method, one can rewrite Eq. (2) as Eq. (10).

$$y_i = w_i = F_i(x)q_i(t) \quad (10)$$

Now using the concept of the lumped mass model (i.e. the lumped parameter method), the kinetic energy of link i due to deformation is replaced by the kinetic energy of m_i numbers of mass, which is described by Eq. (11). Similar to the assumed mode method, the approximation accuracy depends on the number of the mass used to represent a link.

$$\begin{aligned} T_{e,i} &= \frac{1}{2}\rho_i\int_0^{L_i}\dot{w}_i^{\ 2}dx = \frac{1}{2}M_{e,i}\dot{y}_{i,E}^{\ 2} \\ &= \frac{1}{2}\sum_{j=1}^{m_i}\rho_{ij}\int_{(j-1)\ell_i}^{j\ell_i}\dot{w}_{ij}^{\ 2}dx = \frac{1}{2}\sum_{j=1}^{m_i}M_{e,ij}\dot{y}_{ij}^{\ 2} \end{aligned} \quad (11)$$

where y_{ij} is the displacement of the j^{th} mass for link i and notation E represents the endpoint. Each link has m_i numbers of mass, $\ell_i = L_i/m_i$ is the length of each mass, and M_e represents the lumped mass.

Substituting Eq. (10) into Eq. (11) will yield Eq. (12).

$$M_{e,ij} = \frac{\rho_{ij}\int_{(j-1)\ell_i}^{j\ell_i} F_i(x)^2\,dx}{F_i(j\ell_i)^2} \tag{12}$$

One can use Eq. (12) to compute the lumped mass. With the lumped mass $M_{e,ij}$ calculated, one can use Eq. (11) to compute the kinetic energy of the flexible link.

Next, using the concept of the lumped spring model and exploiting Hooke's law, the elastic potential energy can be expressed as Eq. (13)

$$\begin{aligned} U_{e,i} &= \sum_{j=1}^{m}\frac{1}{2}\int_{(j-1)\ell_i}^{j\ell_i} E_{ij}I_{ij}\left(w_{ij}''\right)^2 dx = \sum_{j=1}^{m}\frac{1}{2}K_{e,ij}w_{ij}^2 \\ U_e &= \sum_{i=1}^{n} U_{e,i} \end{aligned} \tag{13}$$

where U_e is the total elastic potential energy, and $U_{e,i}$ is the elastic potential energy of the i^{th} axis.

Let ϕ_i be the deflection angle of the deflection w_i. The indices x, y and z are defined in the right-hand rule, which are described by

$$w_i \cong L_i\phi_i \quad , \quad \phi_i \cong \frac{w_i}{L_i} \cong w_i' = F_i'(x)q_i(t) \tag{14}$$

$$w_{xi} \cong L_i\phi_{yi} \ , \ w_{yi} \cong L_i\phi_{zi} \ , \ w_{zi} \cong L_i\phi_{xi} \tag{15}$$

Substituting Eq. (14) and (15) into Eq. (13) will result in the lumped spring constant of the lumped spring model described by Eq. (16).

$$K_{e,ij} = \frac{E_{ij}I_{ij}}{\ell_i^{\,2}}\frac{\int_{(j-1)\ell_i}^{j\ell_i}\left[F_i''(x)\right]^2 dx}{\left\{F_i'(j\ell_i) - F_i'\left[(j-1)\ell_i\right]\right\}^2} \tag{16}$$

The elastic potential energy of the flexible link for the lumped spring model can be obtained by substituting Eq. (16) into Eq. (13). Now, by substituting the kinetic energy and the potential energy for the flexible part of the flexible link represented in the lumped model into the Euler-Lagrange equation, one can derive the dynamic equation and the flexible deflection that will be elaborated upon later in this paper.

Since only the 1st order assumed mode is used in the above discussion, its computation load is much smaller than the pure assumed mode method.

KINEMATICS OF THE FLEXIBLE ROBOT MANIPULATOR

Forward kinematics of the flexible robot manipulator

The DH parameters are employed in this paper to help derive the forward kinematics of the flexible robot manipulator through a product of a sequence of coordinate transformation matrices (Book, 1979; Chedmail et al., 1991; Yang et al., 2001).

Suppose that (x_i, y_i, z_i) is a coordinate frame established at the i^{th} link and corresponds to the $(i+1)^{\text{th}}$ joint position or the end-effector position. Now, the coordinate transformation matrix for the rigid part of the robot manipulator is described by Eq. (17) (Fu et al., 1987)

$$A_i^{i-1} = \mathrm{Trans}_{z_{n-1}}(d_i)\cdot \mathrm{Rot}_{z_{n-1}}(\theta_i)\cdot \mathrm{Trans}_{x_n}(b_i)\cdot \mathrm{Rot}_{x_n}(\alpha_i) \tag{17}$$

where

$$\begin{cases} \theta_i: \text{angle between } x_{i-1} \text{ and } x_i \text{ that rotates about } z_{i-1} \\ d_i: \text{ distance between } x_{i-1} \text{ and } x_i \text{ along } z_{i-1} \\ \alpha_i: \text{angle between } z_{i-1} \text{ and } z_i \text{ that rotates about } x_i \\ b_i: \text{distance between } z_{i-1} \text{ and } z_i \text{ along } x_i \end{cases}$$

With Eq. (17), the position vector from the end-effector (i.e. endpoint) to the origin as shown in Fig. 3 can be expressed as

$$r_i^0 = A_{i-1}^0 r_i^{i-1} = A_1^0 A_2^1 \cdots A_{i-1}^{i-2} r_i^{i-1} \tag{18}$$

where r_i^{i-1} is the position vector represented in the $(i-1)^{\text{th}}$ coordinate frame that is mapped from the i^{th} coordinate frame and r_i^0 is the position vector represented in the base frame (as indicated by the green solid line in Fig. 3) that is mapped from the i^{th} coordinate frame.

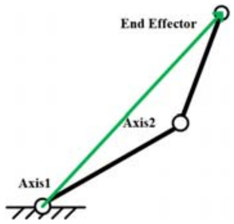

Fig. 3. Forward kinematics for a rigid type 2-link robot manipulator.

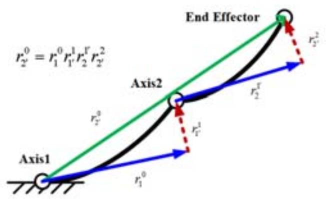

Fig. 4. Forward kinematics for a typical flexible 2-link robot manipulator.

The deflection displacement/angle due to deformation will be derived in a manner similar to the derivation of forward kinematics for the rigid part of the robot manipulator. In particular, the coordinate transformation matrix for the flexible part is described by Eq. (19).

$$E_{i'}^{i} = \begin{bmatrix} R_x(\phi_{xi})R_y(\phi_{yi})R_z(\phi_{zi})\big|_{3\times 3} & w_i\big|_{3\times 1} \\ 0\big|_{1\times 3} & 1 \end{bmatrix} \tag{19}$$

where i' represents the frame after flexibility transformation and

$$R_x(\phi_{xi}) = \begin{bmatrix} 1 & 0 & 0 \\ 0 & \cos\phi_{xi} & -\sin\phi_{xi} \\ 0 & \sin\phi_{xi} & \cos\phi_{xi} \end{bmatrix},\ R_y(\phi_{yi}) = \begin{bmatrix} \cos\phi_{yi} & 0 & \sin\phi_{yi} \\ 0 & 1 & 0 \\ -\sin\phi_{yi} & 0 & \cos\phi_{yi} \end{bmatrix}$$

$$R_z(\phi_{zi}) = \begin{bmatrix} \cos\phi_{zi} & -\sin\phi_{zi} & 0 \\ \sin\phi_{zi} & \cos\phi_{xi} & 0 \\ 0 & 0 & 1 \end{bmatrix},\ w_i = \begin{bmatrix} w_{xi} & w_{yi} & w_{zi} \end{bmatrix}^T.$$

Based on the above coordinate transformation matrix for the flexible part, the position vector from the end-effector to the origin of the base frame is defined to be the position vector represented in the base frame for the rigid part of the robot manipulator plus the deflection (i.e. position deflection displacement) w_i due to deformation. The deflection angles due to deformation (i.e. flexibility) are denoted as ϕ_x, ϕ_y and ϕ_z. By using Eqs. (17)~(20), one can obtain the position vector from the end-effector to the origin of the base frame for the flexible robot manipulator as shown in Fig. 4.

$$r_{i'}^{0} = A_1^0 E_{1'}^{1} \cdots A_{i-1}^{(i-2)'} E_{(i-1)'}^{i-1} r_{i'}^{(i-1)'} \tag{20}$$

There is a restriction when using the coordinate transformation matrix for the flexible part. That is, the origin of a frame must be located at the endpoint of a flexible link if one wants to use the coordinate transformation matrix for the flexible part directly. However, based on the definition of DH parameters, it is possible that the aforementioned requirement will not be satisfied. In order to cope with this difficulty, an auxiliary transformation matrix is employed in this paper. Fig. 5 illustrates the idea of using an auxiliary transformation matrix. In Fig. 5, by following the rule of DH parameters, it is easy to find that Frame 0 and Frame 1 locate at the same point. As a result, there is no frame attached to the endpoint of the first link, so the length of the first link will not appear in the coordinate transformation matrix for the flexibility frame (orange color in Fig. 5). To overcome this difficulty, an auxiliary transformation matrix A_{aux} is employed to move Frame 1 to the endpoint of the second link. With the auxiliary transformation matrix, one can derive the forward kinematics for a flexible robot manipulator using Eq. (21).

$$r_{2'}^{0} = \begin{bmatrix} r_x & r_y & r_z & 1 \end{bmatrix}^T = A_1^0 A_{aux} E_{1'}^{1} r_{2'}^{1'} ,\quad A_{aux} = \begin{bmatrix} 1 & 0 & 0 & 0 \\ 0 & 1 & 0 & 0 \\ 0 & 0 & 1 & L_1 \\ 0 & 0 & 0 & 1 \end{bmatrix} \tag{21}$$

The purpose of the auxiliary transformation matrix A_{aux} in Eq. (21) is to ensure that a frame is attached to a desired position such as the endpoint of a link.

Next we will focus on the derivation of the position vector of the endpoint, i.e. the position vector represented in the i^{th} local frame (the blue vectors in Fig. 4 and Fig. 5). Depending on the type of joints, there are two different representations of the position vector of the endpoint:

$$r_{i'}^{(i-1)'} = \Re_i^{(i-1)'} r_{i'}^{i} \quad , \quad \text{where } \Re_i^{(i-1)'} = \begin{bmatrix} R_i^{(i-1)'} & 0_{3\times1} \\ 0_{1\times3} & 1_{1\times1} \end{bmatrix}$$

(a). The i^{th} joint is a revolute joint

If the x-axis is the rotational axis, then

$$r_{i'}^{i} = r_{i',x}^{i} = \left[\left\{ (w_{xi})\vec{i} + (x + w_{yi})\vec{j} + (w_{zi})\vec{k} \right\}_{3\times1}^{T} \quad 1 \right]^T$$

If the y-axis is the rotational axis, then

$$r_{i'}^{i} = r_{i',y}^{i} = \left[\left\{ (w_{xi})\vec{i} + (w_{yi})\vec{j} + (x + w_{zi})\vec{k} \right\}_{3\times1}^{T} \quad 1 \right]^T$$

If the z-axis is the rotational axis, then

$$r_{i'}^{i} = r_{i',z}^{i} = \left[\left\{ (x + w_{xi})\vec{i} + (w_{yi})\vec{j} + (w_{zi})\vec{k} \right\}_{3\times1}^{T} \quad 1 \right]^T$$

(b). The i^{th} joint is a prismatic joint

Step 1. The z-axis is defined to be the direction of translation: $(x + w_{zi})\vec{k}$.

Step 2. The x-axis (or y-axis) is defined to be perpendicular to the z-axis: $(w_{xi})\vec{i}$.

Step 3. With the z-axis and x-axis (or y-axis) determined, the y-axis (or x-axis) is determined by the right-hand rule: $(w_{yi})\vec{j}$.

$$\Rightarrow \quad r_{i'}^{i} = r_{i',z}^{i} = \left[\left\{ (w_{xi})\vec{i} + (w_{yi})\vec{j} + (x + w_{zi})\vec{k} \right\}_{3\times1}^{T} \quad 1 \right]^T$$

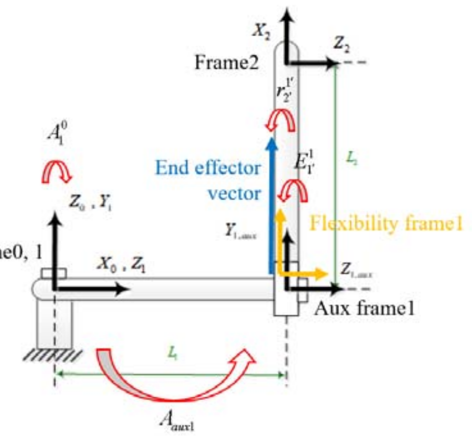

Fig. 5. Illustrative example of using an auxiliary transformation matrix.

The general form of forward kinematics for the flexible robot manipulator can be expressed as Eq. (22)

$$r_{i'}^{0} = T_{(i-1)'}^{0} r_{i'}^{(i-1)'} = \left[A_{aux0} \left(\prod_{j=1}^{i-1} A_j^{j-1} \cdot A_{auxj} \cdot E_{j'}^{j} \right) \right] \Re_i^{(i-1)'} r_{i'}^{i} \tag{22}$$

where the transformation matrix has the following forms

$$\begin{cases} T_{(i-1)'}^{p} = \left[\left(\prod_{j=p+1}^{i-1} A_j^{j-1} \cdot A_{auxj} \cdot E_{j'}^{j} \right) \right] \\ T_{i-1}^{0} = \left[A_{aux0} \left(\prod_{j=1}^{i-2} A_j^{j-1} \cdot A_{auxj} \cdot E_{j'}^{j} \right) A_{i-1}^{(i-2)'} \cdot A_{auxi-1} \right] \\ T_{i-1}^{p} = \left[\left(\prod_{j=p+1}^{i-2} A_j^{j-1} \cdot A_{auxj} \cdot E_{j'}^{j} \right) A_{i-1}^{(i-2)'} \cdot A_{auxi-1} \right] \end{cases}$$

and p is any frame other than the base frame.

Forward velocity kinematics of the flexible robot manipulator

The time derivatives for both the coordinate transformation matrices for the rigid part and flexible part of the flexible robot manipulator are essential in deriving the forward velocity kinematics of the flexible robot manipulator.

$$\dot{A}_i^{(i-1)'} = \begin{cases} \dfrac{\partial A_i^{(i-1)'}}{\partial \theta_i}\dot{\theta}_i = Q_i A_i^{(i-1)'}\dot{\theta}_i = \dot{\mathfrak{R}}_i^{(i-1)'} & \text{revolute} \\ \dfrac{\partial A_i^{(i-1)'}}{\partial d_i}\dot{d}_i = Q_i A_i^{(i-1)'}\dot{d}_i & \text{prismatic} \end{cases} \tag{23}$$

where $Q_i = Q_r$ or Q_d

$$Q_r = \begin{bmatrix} 0 & -1 & 0 & 0 \\ 1 & 0 & 0 & 0 \\ 0 & 0 & 0 & 0 \\ 0 & 0 & 0 & 0 \end{bmatrix}, \quad Q_d = \begin{bmatrix} 0 & 0 & 0 & 0 \\ 0 & 0 & 0 & 0 \\ 0 & 0 & 0 & 1 \\ 0 & 0 & 0 & 0 \end{bmatrix}$$

$$\dot{E}_{i'}^i = \begin{bmatrix} \dfrac{d}{dt}\left(R_x(\phi_x)R_y(\phi_y)R_z(\phi_z)\right)_{3\times3} & 0_{3\times1} \\ 0_{1\times3} & 0_{1\times1} \end{bmatrix}$$
$$= \begin{bmatrix} \begin{pmatrix} \left(Q_x R_x R_y R_z\right)_{3\times3}\dot{\phi}_x + \left(R_x Q_y R_y R_z\right)_{3\times3}\dot{\phi}_y \\ +\left(R_x R_y Q_z R_z\right)_{3\times3}\dot{\phi}_z \end{pmatrix} & 0_{3\times1} \\ 0_{1\times3} & 0_{1\times1} \end{bmatrix} \tag{24}$$

where

$$Q_x = \frac{\partial}{\partial \phi_{xi}} = \begin{bmatrix} 0 & 0 & 0 \\ 0 & 0 & -1 \\ 0 & 1 & 0 \end{bmatrix}, \quad Q_y = \frac{\partial}{\partial \phi_{yi}} = \begin{bmatrix} 0 & 0 & 1 \\ 0 & 0 & 0 \\ -1 & 0 & 0 \end{bmatrix}$$

$$Q_z = \frac{\partial}{\partial \phi_{zi}} = \begin{bmatrix} 0 & -1 & 0 \\ 1 & 0 & 0 \\ 0 & 1 & 0 \end{bmatrix}$$

From Eq. (23) and Eq. (24), the linear velocity of the end-effector to the origin of the base frame is expressed as

$$\dot{r}_{i'}^0 = \frac{d}{dt}\left(T_{(i-1)'}^0 \cdot r_{i'}^{(i-1)'}\right) = V_i\ r_{i'}^i \tag{25}$$

where V_i described by Eq. (26) is the transformation matrix after differentiation, and $p=\theta$ or d.

$$V_i = \left[\sum_{j=1}^{i-1}\begin{pmatrix} T_{(j-1)'}^0 Q_j A_j^{(j-1)'}\dot{p}_j A_{auxj} E_{j'}^j T_{(i-1)'}^{j'}\mathfrak{R}_i^{(i-1)'} \\ +T_{(j-1)'}^0 A_j^{(j-1)'} A_{auxj}^j \dot{E}_{j'}^j T_{(i-1)'}^{j'}\mathfrak{R}_i^{(i-1)'} \end{pmatrix} + T_{(i-1)'}^0 Q_i A_i^{(i-1)'}\dot{\theta}_i\right] \tag{26}$$

The linear velocity can be used to compute the kinetic energy of the flexible robot manipulator.

The derivation of the angular velocity of the end-effector of the flexible robot manipulator will be elaborated upon in the following. Due to the fact that the link of a flexible robot manipulator is not ideally rigid, the velocity of the starting point of a link will not be perfectly synchronized with the velocity of the endpoint of a link. As shown in Fig. 6, the payload for the first link is the actuator (i.e. motor) of the second link. As a result, the angular velocity of the motor is in fact the angular velocity of the payload. In addition, the part colored blue in Fig. 6 represents the bearing of the second link.

In the following discussion, there are two different velocities—the payload angular velocity (for the endpoint of a link) and the hub angular velocity (for the starting point of a link).

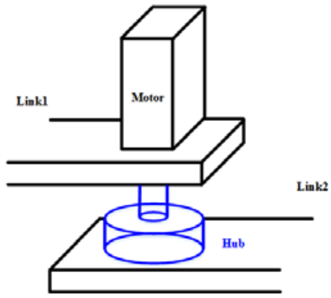

Fig. 6. Linkage between the first link and the second link.

Similar to the derivation of the robot Jacobian for the rigid robot manipulator (Spong et al., 2006), the angular velocity for the hub and the angular velocity for the payload are described by Eq. (27) and Eq. (28), respectively.

$$\omega_{h,i}^0 = \omega_1 + \sum_{j=2}^{i}\left(R_{j-1}^0\dot{\Phi}_{j-1} + \omega_j\right) \tag{27}$$

$$\omega_{p,i}^0 = \sum_{j=1}^{i}\left(R_j^0\dot{\Phi}_j + \omega_j\right) \tag{28}$$

where

$$\dot{\Phi}_i = \begin{bmatrix} \dot{\phi}_{x,i} & \dot{\phi}_{y,i} & \dot{\phi}_{z,i} \end{bmatrix}^T, \quad T_j^0 = \begin{bmatrix} \left(R_j^0\right)_{3\times3} & \left(d_j^0\right)_{3\times1} \\ 0_{1\times3} & 1_{1\times1} \end{bmatrix}$$

$$\omega_j = \begin{cases} \dot{\theta}_j R_{(j-1)'}^0 \hat{u}_j & \text{revolute} \\ \dfrac{\overline{r}_j^0 \times v_j}{\left|\overline{r}_j^0\right|^2}, \quad \text{where } v_j = \dot{d}_j R_{(j-1)'}^0 \hat{u}_j & \text{prismatic} \end{cases}$$

where $r_j^0 = T_{(j-1)'}^0 r_j^{(j-1)'} = T_{(j-1)'}^0 \mathfrak{R}_j^{(j-1)'} r_j^j$, $r_j^j = \left(r_{j'}^j\right)_{rigid}$

Fig. 7 shows the angular velocity for the case of the planar 2-DOF flexible robot manipulator.

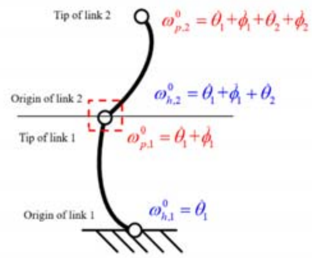

Fig. 7. Angular velocity for the case of the planar 2-DOF flexible robot manipulator.

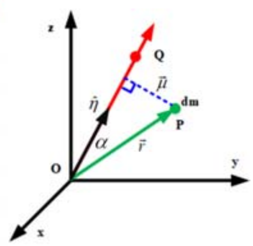

Fig. 8. Moment of inertia for axis OQ.

Moment of inertia in the base frame

Since the Euler-Lagrange equation is employed in this paper to derive the dynamic model, one needs to calculate in advance the kinetic and potential energies associated with moment of inertia for bearings and payloads. In the previous subsection, one can derive the forward velocity kinematics represented in the base frame. In the following, we will derive the moment of inertia for bearings and payloads represented in the base frame so that one can develop the correct formulas for kinetic and potential energies associated with moment of inertia for bearings and payloads in the base frame.

By definition, the moment of inertia for an arbitrary axis OQ shown in Fig. 8 is expressed as

$$I_{OQ} \equiv \int |\mu|^2 \, dm = \int \left(|\vec{r}| \sin\alpha \right)^2 dm = \int |\hat{\eta} \times \vec{r}|^2 \, dm \tag{29}$$

where dm is the infinitesimal mass element, $\hat{\eta} = \begin{bmatrix} \eta_x & \eta_y & \eta_z \end{bmatrix}^T$ is the unit vector in the direction of the OQ axis, $\vec{r} = \begin{bmatrix} x & y & z \end{bmatrix}^T$ is the vector pointing in the direction of point P, and α is the angle between $\hat{\eta}$ and $\vec{r}$.

By expanding Eq. (29), one will have

$$\begin{aligned} &I_{xx} = \int \left(y^2 + z^2 \right) dm, \; I_{yy} = \int \left(x^2 + z^2 \right) dm, \; I_{zz} = \int \left(x^2 + y^2 \right) dm \\ &I_{xy} = -\int xydm, \quad I_{xz} = -\int xzdm, \quad I_{yz} = -\int yzdm \end{aligned} \tag{30}$$

$$I_{OQ} = \eta_x^2 I_{xx} + \eta_y^2 I_{yy} + \eta_z^2 I_{zz} + 2\eta_x\eta_y I_{xy} + 2\eta_x\eta_z I_{xz} + 2\eta_y\eta_z I_{yz} \tag{31}$$

Using Eq. (31), one can convert the moment of inertia represented in the local frame into the moment of inertia represented in the base frame. The procedure is detailed in the following.

Step 1. Assign OQ axis as the *x*-axis, *y*-axis and *z*-axis of the base frame, respectively.
Step 2. The *x*-axis, *y*-axis and *z*-axis of the base frame are converted and represented in a local frame.
Step 3. Calculate the moment of inertia of the base frame.

The above three steps can be described by Eq. (32).

$$\bar{I}_{X,i} = \vec{\eta}_{Xi}^{\,T} I_i \, \vec{\eta}_{Xi}, \quad \bar{I}_{Y,i} = \vec{\eta}_{Yi}^{\,T} I_i \, \vec{\eta}_{Yi}, \quad \bar{I}_{Z,i} = \vec{\eta}_{Zi}^{\,T} I_i \, \vec{\eta}_{Zi} \tag{32}$$

where

$$\begin{cases} \vec{\eta}_{Xi} = \left(R_i^0 \right)^T \hat{i} = \begin{bmatrix} \vec{\eta}_{Xi,x} & \vec{\eta}_{Xi,y} & \vec{\eta}_{Xi,z} \end{bmatrix}^T \\ \vec{\eta}_{Yi} = \left(R_i^0 \right)^T \hat{j} = \begin{bmatrix} \vec{\eta}_{Yi,x} & \vec{\eta}_{Yi,y} & \vec{\eta}_{Yi,z} \end{bmatrix}^T \\ \vec{\eta}_{Zi} = \left(R_i^0 \right)^T \hat{k} = \begin{bmatrix} \vec{\eta}_{Yi,x} & \vec{\eta}_{Zi,y} & \vec{\eta}_{Zi,z} \end{bmatrix}^T \end{cases}, \; I_i = \begin{bmatrix} I_{xx,i} & I_{xy,i} & I_{xz,i} \\ I_{xy,i} & I_{yy,i} & I_{yz,i} \\ I_{xz,i} & I_{yz,i} & I_{zz,i} \end{bmatrix}$$

where I_i is the inertia tensor for the bearing/payload. Note that the local frame for the hub and payload are the same, therefore they have the same inertia tensor formula.

DYNAMICS OF THE FLEXIBLE ROBOT MANIPULATOR

In order to use the Euler-Lagrange equation to derive the dynamic equation that describes the dynamics of the flexible robot manipulator, one must calculate the potential energy and kinetic energy of the flexible robot manipulator in advance.

Energy equation

The energy equation for the flexible robot manipulator is derived based on the existing researches on the assumed modes method and the lumped parameter method. The kinetic energy generated by these components will be dissipated by work due to non-conservative forces such as viscous force and heat. The rest of the energy is due to conservative forces such as gravitational force and spring force that will generate potential energies such as gravitational potential energy and elastic potential energy. In the flexible robot manipulator, in addition to the motor rotor, other components will also contribute gravitational potential energy. In particular, in addition to the potential energy, the link also contains elastic potential energy due to the fact that its rigidity is not high. In order to derive a dynamic model that can faithfully describe the dynamic behaviors of the flexible robot manipulator, this paper will calculate the kinetic energy of the link, kinetic energy of the rotor, kinetic energy of the hub/payload, elastic potential energy of the link, gravitational potential energy of the link, and gravitational potential energy of the hub/payload. In the following, a lumped parameter-based approach will be exploited to study these energies, in which a single link is approximated by a set of lumped parameters.

Firstly, we will calculate the kinetic energy of the link. According to (Meirovitch, 1988), the kinetic energy of any point mass on the robot manipulator is calculated using the time derivative of the position vector in the base frame. By definition, the sum of the kinetic energy of all point masses is the kinetic energy of the whole system. As a result, the kinetic energy T_{link} for all links in a flexible robot manipulator can be expressed as

$$T_{link} = \frac{1}{2} \sum_{i=1}^{n} \int_0^{L_i} \rho_i(\xi) \left[\dot{r}_i^0(\xi) \right]^T \left[\dot{r}_i^0(\xi) \right] d\xi \tag{33}$$

where n is the total number of links in a flexible robot manipulator, and index i is the i^{th} link.

By following the derivation process of the dynamic equation for a rigid robot manipulator in (Fu et al., 1987), the investigation of the kinetic energy of a link is divided into the rigid part and the flexible part in this paper. In particular, the kinetic energy of the flexible part is derived using the lumped parameter method. That is, the kinetic energy of the flexible part can be regarded as if it were generated by a virtual mass. By satisfying the assumption described by Eq. (15), deviations due to deformation w_x, w_y, w_z, can be expressed in the form of $L\phi_x$, $L\phi_y$, $L\phi_z$, respectively. As a result, one can rewrite Eq. (33) into Eq. (34) as

$$T_{link} = \frac{1}{2} \sum_{i=1}^{n} \left\{ Trace\left(V_i J_i V_i^T \right) + M_{e,i} L_i \left(\dot{\Phi}_i^T \dot{\Phi}_i + \dot{P}_i^T \dot{P}_i \right) \right\} \tag{34}$$

where

$$\left(\dot{r}_{i'}^0 \right)_{rigid} = V_i \left(r_{i'}^i \right)_{rigid}, \quad \left(r_{i'}^i \right)_{rigid} = \left(r_{i'}^i \right) \Big|_{w_x = w_y = w_z = 0}$$

$$M_{e,i} = \begin{bmatrix} M_{e,xi} & M_{e,yi} & M_{e,zi} \end{bmatrix}, \quad \dot{\Phi}_i^T = \begin{bmatrix} \dot{\phi}_{x,i} & \dot{\phi}_{y,i} & \dot{\phi}_{z,i} \end{bmatrix}^T$$

$$\dot{P}_i=\begin{cases}\left(R^T\Big|_{E^i_{i'}}\right)\left(R^T\Big|_{A_i^{(i-1)'}}\right)\dot{\theta}_i\hat{u} & \text{, revolute joint}\\ 0 & \text{, prismatic joint}\end{cases}$$

$$J_i=\int_0^{L_i}\rho_i(\xi)\left[r^i_{i'}\right]_{rigid}\left[r^i_{i'}\right]^T_{rigid}d\xi\ ,$$

and $J_i=J_{i,x}$ or $J_{i,y}$ or $J_{i,z}$

$R\Big|_{E^i_{i'}}$ is the rotation matrix R in $E^i_{i'}$

$R\Big|_{A_i^{(i-1)'}}$ represents the rotation matrix R in $A_i^{(i-1)'}$

$$J_{i,x}=\begin{bmatrix}\int_0^{L_i}\rho_{i,x}(\xi)\xi^2d\xi & 0 & 0 & \int_0^{L_i}\rho_{i,x}(\xi)\xi d\xi\\ 0 & 0 & 0 & 0\\ 0 & 0 & 0 & 0\\ \int_0^{L_i}\rho_{i,x}(\xi)\xi d\xi & 0 & 0 & \int_0^{L_i}\rho_{i,x}(\xi)d\xi\end{bmatrix}$$

$$J_{i,y}=\begin{bmatrix}0 & 0 & 0 & 0\\ 0 & \int_0^{L_i}\rho_{i,y}(\xi)\xi^2d\xi & 0 & \int_0^{L_i}\rho_{i,y}(\xi)\xi d\xi\\ 0 & 0 & 0 & 0\\ 0 & \int_0^{L_i}\rho_{i,y}(\xi)\xi d\xi & 0 & \int_0^{L_i}\rho_{i,y}(\xi)d\xi\end{bmatrix}$$

$$J_{i,z}=\begin{bmatrix}0 & 0 & 0 & 0\\ 0 & 0 & 0 & 0\\ 0 & 0 & \int_0^{L_i}\rho_{i,z}(\xi)\xi^2d\xi & \int_0^{L_i}\rho_{i,z}(\xi)\xi d\xi\\ 0 & 0 & \int_0^{L_i}\rho_{i,z}(\xi)\xi d\xi & \int_0^{L_i}\rho_{i,z}(\xi)d\xi\end{bmatrix}$$

Secondly, the kinetic energy of the rotor can be expressed as

$$T_{rotor}=\frac{1}{2}\sum_{i=1}^{n}I_{r,i}\left(\gamma_i^2\dot{\theta}_i^2\right) \tag{35}$$

where γ_i is the moment of inertia of the rotor.

As for the calculations of kinetic energy for the hub and payload, one can apply Konig's theorem described by Eq. (36). Similar to the case of a link, the kinetic energy of a system is equivalent to the sum of the kinetic energy of all point masses of the system. It is also equivalent to the sum of the kinetic energy of the center of mass for conducting a translational motion and the kinetic energy of the moment of inertia relative to the center of mass of the system for conducting a rotational motion.

$$\begin{aligned}K_{total}&=\sum_{i=1}^{n}K_i=\sum_{i=1}^{n}\frac{1}{2}m_iv_i^{\,2}=\frac{1}{2}M_{total}v_c^{\,2}+\sum_{i=1}^{n}\frac{1}{2}m_iv_{ic}^{\,2}\\&=\frac{1}{2}M_{total}v_c^{\,2}+\frac{1}{2}\mathrm{I}_c\omega^2\\&=\text{kinetic energy of translation and rotation}\end{aligned} \tag{36}$$

where notation "c" represents "center of mass".

Similar to the above discussions, the calculation of kinetic energy of hub and payload is also divided into two parts—kinetic energy due to translational motion and kinetic energy due to rotational motion.

As for the case of kinetic energy due to translational motion, in this paper it is assumed that the hub of the i^{th} axis and the payload of the $(i-1)^{th}$ axis have the same center of mass. Therefore, the sum of their kinetic energies due to translational motion is equivalent to the kinetic energy due to translational motion of the sum of these two masses. As a result, to simplify, one can combine these two cases as described by Eq. (37):

$$\begin{aligned}T_{hub,mass}+T_{payload,mass}&=\frac{1}{2}\sum_{i=1}^{n}\left(M_{p,i}+M_{h,i+1}\right)\dot{r}^0_{i'}(L_i)^T\cdot\dot{r}^0_{i'}(L_i)\\&=\frac{1}{2}\sum_{i=1}^{n}\left(M_{p,i}+M_{h,i+1}\right)r^i_{i'}(L_i)^T\,V_i^T\,V_i\,r^i_{i'}(L_i)\end{aligned} \tag{37}$$

Note that there is no kinetic energy due to translational motion for the hub of the 1st axis, while there is no kinetic energy due to rotational motion for the last axis.

As mentioned in Section 3, the rotational velocity of the hub and the rotational velocity of the payload are not the same. Therefore, the kinetic energy due to rotational motion for the case of the hub and that for the case of the payload will be discussed separately. Using Eq. (27), Eq. (28) and Eq. (32), one can obtain

$$T_{hub,inertia}=\frac{1}{2}\sum_{i=1}^{n}\overline{I}_{h,i}\left(\omega^{0\ \circ 2}_{h,i}\big|_{3\times 1}\right) \tag{38}$$

$$T_{payload,inertia}=\frac{1}{2}\sum_{i=1}^{n}\overline{I}_{p,i}\left(\omega^{0\ \circ 2}_{p,i}\big|_{3\times 1}\right) \tag{39}$$

where T_{hub} is the kinetic energy of the hub due to rotational motion and $T_{payload,inertia}$ is the kinetic energy of the payload due to rotational motion. In addition, $\overline{I}_{h,i}=\left[\overline{I}_{hx,i}\quad\overline{I}_{hy,i}\quad\overline{I}_{hz,i}\right]$, $\overline{I}_{p,i}=\left[\overline{I}_{px,i}\quad\overline{I}_{py,i}\quad\overline{I}_{pz,i}\right]$. 「$\circ$」 is called the Hadamard product (i.e. the entrywise product), in which

$$\begin{cases}\left(\omega^{0\ \circ 2}_{h,i}\right)=\left[\omega^{0\ 2}_{hx,i}\quad\omega^{0\ 2}_{hy,i}\quad\omega^{0\ 2}_{hz,i}\right]^T\\ \left(\omega^{0\ \circ 2}_{p,i}\right)=\left[\omega^{0\ 2}_{px,i}\quad\omega^{0\ 2}_{py,i}\quad\omega^{0\ 2}_{pz,i}\right]^T\end{cases}$$

The elastic potential energy and the gravitational potential energy for the flexible robot manipulator will be elaborated in the following. We will start with the calculation of the elastic potential energy for the link. Similar to the discussion on the kinetic energy of the link, the elastic potential energy for each link is described by a lumped spring model as shown in Eq. (40).

$$U_{elastic}=\frac{1}{2}\sum_{i=1}^{n}\left[K_iL_i^{\,2}\Phi_i^{\circ 2}\right] \tag{40}$$

where $K_i=\left[K_{e,xi}\quad K_{e,yi}\quad K_{e,zi}\right]$

Finally, we will calculate the gravitational potential energy. Since the deviation due to flexibility is very small for a link, in this paper only the gravitational potential energy of the link due to rigidity will be discussed. Its general expression is described by Eq. (41):

$$U_{gravity,link} \approx \sum_{i=1}^{n}\left\{\int_0^{L_i} \rho_i(x_i)\,\vec{g}\left(r_{i'}^0(x_i)_{rigid}\right)dx\right\} = \sum_{i=1}^{n}\left\{\vec{g}T_{(i-1)'}^0\,\Re_i^{(i-1)'}\delta_i\right\} \quad (41)$$

where $\delta_i = \int_0^{L_i} \rho_i(\xi)\left[r_{i'}^i\right]_{rigid} d\xi$, $\delta_i = \delta_{i,x}$ or $\delta_{i,y}$ or $\delta_{i,z}$

$$\delta_{i,x} = \left[\int_0^{L_i} \rho_{i,x}(\xi)\,\xi d\xi \quad 0 \quad 0 \quad \int_0^{L_i} \rho_{i,x}(\xi)\,d\xi\right]^T$$

$$\delta_{i,y} = \left[0 \quad \int_0^{L_i} \rho_{i,y}(\xi)\,\xi d\xi \quad 0 \quad \int_0^{L_i} \rho_{i,y}(\xi)\,d\xi\right]^T$$

$$\delta_{i,z} = \left[0 \quad 0 \quad \int_0^{L_i} \rho_{i,z}(\xi)\,\xi d\xi \quad \int_0^{L_i} \rho_{i,z}(\xi)\,d\xi\right]^T$$

$\vec{g} = \vec{g}_x$ or $\vec{g}_y$ or $\vec{g}_z$

$\vec{g}_x = \left[|g| \quad 0 \quad 0 \quad 0\right]$, $\vec{g}_y = \left[0 \quad |g| \quad 0 \quad 0\right]$,

$\vec{g}_z = \left[0 \quad 0 \quad |g| \quad 0\right]$

As mentioned previously, it is assumed that the hub of the i^{th} axis and the load of the $(i-1)^{th}$ axis have the same center of mass. As a result, to simplify, one can combine these two cases as described by Eq. (42):

$$U_{gravity,hub} + U_{gravity,payload} = \sum_{i=1}^{n}\left(m_{h,i+1} + m_{p,i}\right)\vec{g}\,r_{i'}^0(L_i) = \sum_{i=1}^{n}\left(m_{h,i+1} + m_{p,i}\right)\vec{g}\,T_{(i-1)'}^0\,\Re_i^{(i-1)'}r_{i'}^i(L_i) \quad (42)$$

Note that there is no gravitational potential energy for the hub of the 1st axis and the last axis.

Derivation of the dynamic equation for a flexible robot manipulator

Substituting all the kinetic energies and potential energies derived in Section 4.1 into the Lagrangian L of the Euler-Lagrange equation described by Eq. (43), one can derive the dynamic equation of the flexible robot manipulator based on the lumped parameter method:

$$\tau_k = \frac{d}{dt}\frac{\partial L}{\partial \dot{p}_k} - \frac{\partial L}{\partial p_k},\ 0 = \frac{d}{dt}\frac{\partial L}{\partial \dot{\phi}_{xk}} - \frac{\partial L}{\partial \phi_{xk}},\ k = 1,2,\cdots,n$$
$$0 = \frac{d}{dt}\frac{\partial L}{\partial \dot{\phi}_{yk}} - \frac{\partial L}{\partial \phi_{yk}},\ 0 = \frac{d}{dt}\frac{\partial L}{\partial \dot{\phi}_{zk}} - \frac{\partial L}{\partial \phi_{zk}} \quad (43)$$

where k denotes the k^{th} link in an n-DOF flexible robot manipulator.

Since the kinematic energy terms and the potential energy terms contained in the Lagrangian L are decoupled, one can substitute the kinematic energy and the potential energy term by term into the Eq. (43) to yield eight dynamic equations in total for the flexible robot manipulator. Each dynamic equation consists of inertia force, Coriolis force, centrifugal force, gravitational force and spring force. By rewriting these eight dynamic equations into a matrix form, one can obtain Eq. (44):

$$\begin{bmatrix}\tau_{n\times1}\\ 0_{3n\times1}\end{bmatrix} = \underbrace{M(Q)_{4n\times4n}\ddot{Q}_{4n\times1}}_{\text{Inertia force}} + \underbrace{C(Q,\dot{Q})_{4n\times1}}_{\text{Coriolis and centrifugal force}} + \underbrace{G(Q)_{4n\times1}}_{\text{Gravity force}} + \underbrace{D_{4n\times4n}\dot{Q}_{4n\times1}}_{\text{Damping force}} + \underbrace{K_{4n\times4n}Q_{4n\times1}}_{\text{Spring force}} \quad (44)$$

where $Q = \left[p_{n\times1} \quad \phi_{x,n\times1} \quad \phi_{y,n\times1} \quad \phi_{z,n\times1}\right]^T$.

Note that by removing the flexible part of the robot manipulator, Eq. (44) can be also used to derive the dynamic model for the rigid robot manipulator.

SIMULATIONS AND EXPERIMENTAL RESULTS

In order to verify the effectiveness of the proposed approach, a single-link flexible robot manipulator is adopted in the simulation performed using MATLAB. In addition, the real experiment of the single-link flexible robot manipulator is also conducted. Note that in all simulations, the gear ratio γ is set to 50. In addition, a PD-like control law described by Eq. (45) is adopted and the corresponding control block diagram is shown in Fig. 9.

$$\tau_{cmd} = K_{pv}\left[K_{pp}\left(p_{cmd} - p\right) - \dot{p}\right] \quad (45)$$

where K_{pp}=70, K_{pv}=50.

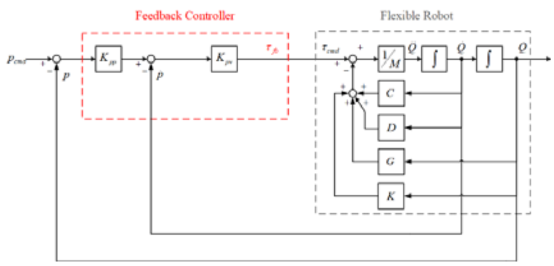

Fig. 9. Control block diagram of the flexible robot manipulator used in all simulations.

Single-link flexible robot manipulator

A single-link flexible robot manipulator provided by Delta Electronics Inc. shown in Fig. 10 is used as the experimental platform. In the experiment, the frequency domain analysis approach is employed to obtain the natural frequency of the flexible robot manipulator. The obtained results are compared with the results obtained using the lumped parameter method to verify the validity of the dynamic model derived using the proposed approach. Table 1 shows the system parameters of the single-link flexible robot manipulator used in the experiment, in which the joint is actuated by a 400W Delta AC servomotor (ECMC-CW0604).

The frequency response of the actuator (i.e. driven oscillator) for the single-link flexible robot manipulator shown in Fig. 11 has an anti-resonance frequency around 8.24 Hz, which indicates that the natural frequency (i.e. resonance) of the single-link flexible robot manipulator is around 8.24 Hz (Belbasi et al., 2014). Subsequently, the proposed approach is used in the simulation (system parameters are listed in Table 1). After calculation, the lumped mass is 0.008634 kg and the lumped spring constant is 96.7425 kg/s^2. Since the moment of inertia of the rotor and gear ratio are irrelevant to the natural frequency of the link, their values are set to $I_{\gamma 1}$=0.002 kg·m^2 and γ_1=50, while the damping coefficient ξ_1 is set to 0.0005. A step response that corresponds to the position input of the motor from 10° to 30° is conducted. The initial deformation angle is assumed to be zero. The simulation results for all three directions are shown in Fig. 12. The primary vibration direction in the simulation is the *z*-axis. The step response ϕ_z shown in Fig. 12 (e) indicates that the natural frequency of the link is around 1/(1.963sec–1.845sec)=8.4745Hz. The comparison between the natural frequency obtained from the real single-link flexible robot manipulator experiment and that of the simulation is listed in Table 4. In addition, from ϕ_x shown in Fig. 12 (a) (*x*-axis is the primary drooping direction), one can find that there is almost no deformation occurring due to its extremely high rigidity, 248 N·m^2. Table 2 also indicates that the discrepancy between the natural frequency obtained from the real single-link flexible robot manipulator experiment and that of the simulation is very small. It suggests that the accuracy of the dynamic model of the single-link flexible robot manipulator obtained using the proposed approach is satisfactory.

Fig. 10. Single-link flexible robot manipulator used in the experiment.

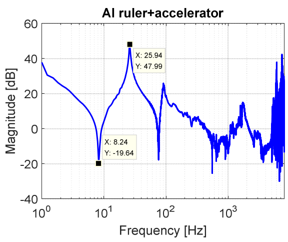

Fig. 11. Frequency response of the actuator of the single-link flexible robot manipulator.

In addition, the commonly used assumed mode approach is also employed to derive the dynamic model of the single-link flexible robot manipulator. In particular, the 2nd order assumed mode method is used in the computer simulation, for which the system parameters used in the simulation are listed in Table 3. Since the primary concern is the motion in the *z*-axis direction, therefore the motion related to the other two dimensions is ignored. In the simulation, the initial position is set to $\theta_1 = 10^0$, $w_{y1} = L_1\phi_{z1} = 0$.

Table 1. System parameters of the single-link flexible robot manipulator

Link length L_1	0.28 m	Payload mass M_{p1}	0.025607 kg
Line density ρ_1	0.1289 kg/m	Rigidity of link $E_{x1}I_{x1}$	248 N·m^2
Rigidity of link $E_{y1}I_{y1}$	0.70656 N·m^2	Rigidity of link $E_{z1}I_{z1}$	0.70656 N·m^2

$$I_{h1} = \begin{bmatrix} 0.00003 & 0 & 0 \\ 0 & 0.00023 & 0 \\ 0 & 0 & 0.00023 \end{bmatrix} \mathrm{kg \cdot m^2}$$

$$I_{p1} = \begin{bmatrix} 0 & 0 & 0 \\ 0 & 0 & 0 \\ 0 & 0 & 4.7575\times10^{-7} \end{bmatrix} \mathrm{kg \cdot m^2}$$

Table 2. Comparison between the natural frequency obtained from the experiment and that of the simulation

	Real experiment	Simulation	Discrepancy
Natural frequency	8.24 Hz	8.4745 Hz	2.767 %

Table 3. System parameters of single-link flexible robot manipulator for the 2nd order assumed mode method

Link length L_1	1.0 m	Moment of inertia of rotor I_{r1}	0.002 kg·m^2
Line density ρ_1	0.1 kg/m	Damping coefficient ξ_1	0.1
Rigidity of link E_1I_1	2.0 N·m^2	Payload mass M_{p1}	0.2 kg

$$I_{h1} = \begin{bmatrix} 0.2 & 0.001 & 0.001 \\ 0.001 & 0.2 & 0.001 \\ 0.001 & 0.001 & 0.2 \end{bmatrix},\ I_{p1} = \begin{bmatrix} 0.001 & 0.001 & 0.001 \\ 0.001 & 0.001 & 0.001 \\ 0.001 & 0.001 & 0.001 \end{bmatrix} \text{ unit: kg}\cdot\text{m}^2$$

Table 4. Simulation results (assumed mode method vs. lumped parameter method)

	2nd order assumed mode	lumped parameter	Discrepancy
Natural frequency	0.7937 Hz	0.813 Hz	2.374%
Amplitude	0.1462 m	0.2032 m	28.05%

Table 5. Comparison of computation time (assumed mode method vs. lumped parameter method)

	2nd order assumed mode	lumped parameter	Computation time ratio
Kinematics	2.633 sec	1.323 sec	50.25 %
Dynamics	6.841 sec	4.047 sec	59.16 %
Constant torque command	36.860 sec	23.442 sec	64.60 %
Feedback control	36.894 sec	23.605 sec	63.98 %

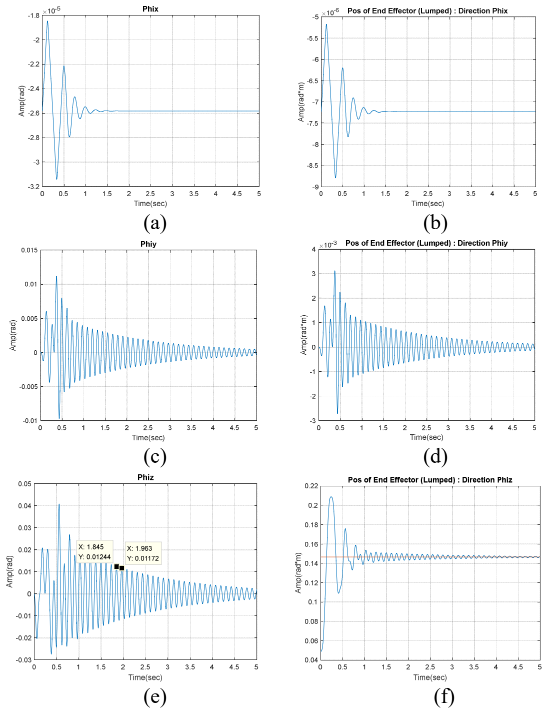

Fig. 12. Simulation of step response corresponding to the position input of the motor from 10° to 30° (a) ϕ_x (b) w_x (c) ϕ_y (d) w_y (e) ϕ_z (f) w_z

The simulation results shown in Fig. 13 and Table 4 indicates that the discrepancy between the natural frequency obtained using the proposed approach and that using the second order assumed mode method is very small, while the discrepancy in amplitude is slightly less than 30%. That is, the system characteristics predicted using these two methods are similar. According to Table 5, the computation time for the proposed approach is smaller than that for the second order assumed mode method.

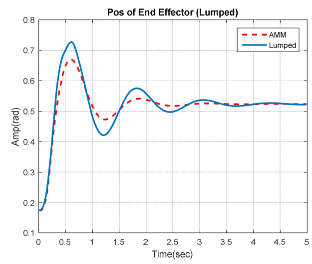

Fig. 13. Simulation results of feedback control (assumed mode method vs. lumped parameter method).

CONCLUSIONS

This paper employs the lumped parameter method to derive the mathematical model of the flexible robot manipulator. The energy equation, kinematics model and dynamic model of the flexible robot manipulator derived using the proposed approach are in general form. Namely, these equations and models are suitable for arbitrary configurations of links, rotational and translational motions and any number of axes. If the flexible part is removed, all the equations and models derived using the proposed approach will degenerate into those for rigid robot manipulators. Simulations and experimental results verify the effectiveness of the proposed approach. Since the proposed approach does not involve any terms that require real integration of deformation due to flexibility, its computation load is reasonable.

REFERENCES

Belbasi, S., Foulaadv, M.E. and Joe, Y.S., “Anti-resonance in a One-dimensional Chain of Driven Coupled Oscillators,” Am. J. Phys., Vol.82, No.1, pp.32-38 (2014)

Benati, M. and Morro, A., “Dynamics of Chain of Flexible Links,” J. Dyn. Syst. Meas. Control Vol.110, No.4, pp.410-415 (1988)

Book, W. J., “Analysis of Massless Elastic Chains with Servo Controlled Joints,” J. Dyn. Syst. Meas. Control, Vol.101, No.3, pp.187-192 (1979)

Book, W.J., “Modeling, Design, and Control of Flexible Manipulator Arms: A Tutorial Review,” In Proceedings of the 29th IEEE Conference on Decision and Control, Honolulu, HI, USA, Dec. 5-7, pp.500-506 (1990)

Chapnik, B.V., Heppler, G.R. and Aplevich, J.D., “Modeling Impact on a One-link Flexible Robotic Arm,” IEEE Trans. Robot. Autom., Vol.7, No.4, pp.479-488 (1991)

Chedmail, P., Aoustin, Y. and Chevallereau, C., “Modelling and Control of Flexible Robots,” Int. J. Numer. Metho. Eng., Vol.32, No.8, pp.1595-1619 (1991)

Denavit, J. and Hartenberg, R.S., “A Kinematic Notation for Lower-pair Mechanisms Based on Matrices,” J. Appl. Mech., Vol.23, pp.215-221 (1955)

Dwivedy, S.K. and Eberhard, P., “Dynamic Analysis of Flexible Manipulators, a Literature Review,” Mech. Mach. Theory, Vol.41, No.7, pp.749-777 (2006)

Faris, W.F., Ata, A.A. and Sa’adeh, M.Y., “Energy Minimization Approach for a Two-link Flexible Manipulator, J. Vibr. Control, Vol.15, No.4, pp.497-526 (2009)

Feliu, V., Rattan, K.S. and Brown, H.B. Jr., “Modeling and Control of Single Link Flexible Arms with Lumped Masses,” J. Dyn. Syst. Meas. Control, Vol.114, No.1, pp.59-69 (1992)

Fu, K.S., Gonzalez, R. C. and Lee, C.S.G., Robotics: Control, Sensing, Vision, and Intelligence, McGraw-Hill Book Company, New York, U.S.A. (1987)

Gao, Y. and Wang, F.Y., Flexible Manipulators Modeling, Analysis and Optimum Design,

Academic Press, Portland, U.S.A. (2012)
Ge, S.S., Lee, T.H. and Zhu, G., "A New Lumping Method of a Flexible Manipulator," In Proceedings of the 1997 American Control Conference, Albuquerque, NM, USA, June 6-6, pp.1412-1416 (1997)
Hastings, G.G. and Book, W.J., "A Linear Dynamic Model for Flexible Robotic Manipulators," IEEE Contr. Syst. Magazine, Vol.7, No.1, pp.61-64 (1987)
Hong, J., He, W., Li, Z. and Zhang, S., "Vibration Control and Angular Tracking of a Flexible Link via Neural Networks," In Proceedings of the 27th Chinese Control and Decision Conference, Qingdao, China, May 23-25, pp. 2951-2956 (2017)
Lochan, K., Roy, B.K. and Subudhi, B., "A Review on Two-link Flexible Manipulators," Ann. Rev. Control, Vol.42, pp.346-367 (2016)
Luca, A.D. and Siciliano, B., "Closed-form Dynamic Model of Planar Multilink Lightweight Robots," IEEE Trans. Sys. Man Cybern., Vol.21, No.4, pp.826-839 (1991)
Martins, J.M., Mohamed, Z., Tokhi, M.O., Costa, J.S.D. and Botto, M.A., "Approaches for Dynamic Modelling of Flexible Manipulator Systems," IEE Proceedings, Contr. Theory Applica., Vol.150, No.4, pp.401-411 (2003)
Matsuno, F., Asano, T. and Sakawa, Y., "Modeling and Quasi-static Hybrid Position/force Control of Constrained Planar Two-link Flexible Manipulators," IEEE Trans. Robot. Autom., Vol.10, No.3, pp.287-297 (1994)
Meirovitch, L., Methods of Analytical Dynamics, McGraw-Hill Book Company, New York, U.S.A. (1988)
Meirovitch, L., Principle and Techniques of Vibrations, Prentice-Hall, New Jersey, U.S.A (1997)
Meng, D., She, Y., Xu, W., Lu, W. and Liang, B., "Dynamic Modeling and Vibration Characteristics Analysis of Flexible-link and Flexible-joint Space Manipulator," Multibody Syst. Dyn., Vol.43, pp.321–347 (2018)
Sakawa, Y., Matsuno, F. and Fukushima, S., "Modeling and Feedback Control of a Flexible Arm," J. Robot. Syst. Vol.2, No.4, pp.452-472 (1985)
Sharifnia, M. and Akbarzadeh, A., "A Constrained Assumed Modes Method for Dynamics of a Flexible Planar Serial Robot with Prismatic Joints," Multibody Syst. Dyn., Vol.40, pp.261–285 (2017)
Spong, M. W., Hutchinson, S. and Vidyasagar, M., Robot Modeling and Control, John Wiley & Sons, New York, U.S.A. (2006)
Subudhi, B. and Morris, A.S., "Dynamic Modelling, Simulation and Control of a Manipulator with Flexible Links and Joints," Robot. Auton. Syst., Vol.41, No.4, pp.257-270 (2002)
Sun, C., He, W. and Hong, J., "Neural Network Control of a Flexible Robotic Manipulator Using the Lumped Spring-mass Model," IEEE Trans. Syst. Man Cybern.: System, Vol.47, No.8, pp.1863-1874 (2017)
Theodore, R.J. and Ghosal, A., "Comparison of the Assumed Modes and Finite Element Models for Flexible Multi-link Manipulators," Int. J. Robot. Resea., Vol.14, No.2, pp.91-111 (1995)
Tokhi, M. O. and Azad, A.K.M., Flexible Robot Manipulators Modelling, Simulation and Control, The Institution of Engineering and Technology, London, U.K. (2008)
Yang, T. W., Xu, W.L. and Tso, S.K., "Dynamic Modeling Based on Real-time Deflection Measurement and Compensation Control for Flexible Multi-link Manipulators," Dyna. Control, Vol.11, No.1, pp.5-24 (2001)
Zhang, X., Mills, J. K. and Cleghorn, W.L., "Dynamic Modeling and Experimental Validation of a 3-PRR Parallel Manipulator with Flexible Intermediate Links," J Intell Robot Syst, Vol.50, pp.323–340 (2007)
Zhu, G., Ge, S.S. and Lee, T.H., "Simulation Studies of Tip Tracking Control of a Single-link Flexible Robot Based on a Lumped Model," Robotica, Vol.17, No.1, pp.71-78 (1999)

基於集總參數法之細長桿件撓性機械手臂建模研究

許忠湛　黃浩倫　魯昶甫　鄭銘揚
國立成功大學電機工程學系

摘 要

撓性桿件機械手臂係以較輕且剛性較低之材質製成。低剛性特性使其在操作上較剛性機械手臂安全，然而也導致撓性桿件容易產生末端點振動問題。因此相較於剛性機械手臂，撓性桿件機械手臂之運動精度通常較差。有鑒於基於模型之控制架構為解決振動問題之一有效方法，本文使用 Euler-Bernoulli 方程式、Euler-Lagrange 方程式以及集總參數法等方法，針對具細長撓性桿件之機械手臂之數學模型推導進行深入研究。我們已進行數個實驗及電腦模擬。實驗結果顯示，真實單一撓性桿件機械手臂之自然振動頻率與本文所推導之數學模型之自然振動頻率相近。另外電腦模擬亦顯示本文所提方法確實有效。